American Mineralogist, Volume 83, pages 339–347, 1998

High-temperature multi-nuclear NMR investigation of analcime

YEONGKYOO KIM AND R. JAMES KIRKPATRICK*

Department of Geology, University of Illinois, Urbana, Illinois 61801, U.S.A.

ABSTRACT

Two analcimes of hydrothermal and diagenetic origin were investigated by in situ ^{29}Si, ^{27}Al, and ^{23}Na NMR from room temperature to 550 °C, and by TGA and DSC. The two samples dehydrate at different temperatures, and the high-temperature NMR behavior is closely related to the dehydration. The diagenetic analcime (CR-6) has higher surface area, and thus its dehydration starts and is completed at lower temperatures than the hydrothermal analcime (Hilaire). The ^{29}Si chemical shifts and ^{27}Al peak maxima become first more shielded and then less shielded with increasing temperature and are related to changes in the Si-O-Si and Si-O-Al bond angles caused by thermal expansion, distortion of framework due to H_2O loss at high temperature, and the decreased bond length caused by rigid unit modes (RUMs). Changes in the ^{27}Al NMR peak widths are also correlated to H_2O loss at high temperature and are due to the increased mobilities of H_2O and Na. Paramagnetic impurities and motion of H_2O and Na play important roles in the T_1 relaxation of ^{27}Al. The ^{23}Na NMR peak maxima become first more negative and then less negative with increasing temperature, with the most negative values occurring near the temperature of maximum H_2O loss. The ^{23}Na peak width decreases, increases, and then again decreases with increasing temperature. These results are best interpreted as due to Na undergoing exchange between the 24(c) Na sites and other sites, possibly the 16(b) H_2O sites, combined with collapse of the cages. The less negative ^{23}Na peak and increasing and then decreasing ^{23}Na peak widths at high temperature are due to the effects of motional averaging of the intensity due to the ($\pm$½, $^3/_2$) satellite transitions.

INTRODUCTION

Analcime ($NaAlSi_2O_6 \cdot H_2O$) is the smallest-pore zeolite and occurs widely in hydrothermal and diagenetic environments (Gottardi and Galli 1985). Hydrothermal analcimes normally have a composition very close to the stoichiometric formula (Si/Al = 2), but sedimentary analcimes have Si/Al ranging from 2 to 3 (Gottardi and Galli 1985).

The cation and H_2O mobilities in the analcime cages are low for a zeolite, and thus it is a possible candidate for the storage of radioactive waste (Dyer and Molyneux 1968; Dyer and Yusof 1987 1989; Todorović et al. 1987a, 1987b; Garney 1992). Thus, study of the high-temperature structural and dynamic behavior of Na in analcime and their relationships to H_2O content is of both geological and technological importance. This paper presents the results of an investigation of analcime that combines high-temperature ^{29}Si, ^{27}Al, and ^{23}Na nuclear magnetic resonance spectroscopy (NMR), thermogravimetric analysis (TGA), and differential scanning calorimetry (DSC), focusing on the changes in the aluminosilicate framework and the local environments and mobility of Na.

The crystal structure of analcime was one of the first zeolites to be determined (Taylor 1930), and it has been refined many times since (Knowles et al. 1965; Ferraris et al. 1972; Mazzi and Galli 1978). Its ideal crystal structure is composed of 16 formula units in a cubic unit cell (space group *Ia*3*d*), with a random distribution of 16 Al and 32 Si atoms on the 48(g) tetrahedral positions and a random distribution of 16 Na atoms on the 24(c) channel positions. Framework O atoms are in 96(h) general positions, and the O atoms of the H_2O molecules are in 16(b) channel positions. Framework O atoms are shared between linked (Si,Al) tetrahedra to form an aluminosilicate framework composed of rings of six and four tetrahedra. The H_2O molecules are confined to channels within this framework, and the Na ions are coordinated by four framework O atoms and two H_2O molecules. As the silica content increases, the Na content decreases, and there is a concurrent linear increase in the number of H_2O molecules (Breck 1984). This structure is similar to that of leucite ($KAlSi_2O_6$), which is tetragonal with space group $I4_1/a$ at room temperature (Mazzi et al. 1976; Hellner and Koch 1979). The only difference is that the larger K atoms in leucite occupy the H_2O 16(b) positions of analcime, instead of the Na 24(c) positions.

There have been few NMR studies of analcime, and only ^{29}Si NMR spectra have been reported (Murdoch et al. 1988; Phillips and Kirkpatrick 1994; Kohn et al. 1995). The published room temperature results are fully

* E-mail: kirkpat@hercules.geology.uiuc.edu

0003–004X/98/0304–0339$05.00

TABLE 1. Chemical compositions of the CR-6 and Hilaire analcime samples as determined by XRF methods

	SiO_2	Al_2O_3	Fe_2O_3 (T)	MgO	CaO	K_2O	Na_2O	P_2O_5	TiO_2	LOI	Sum
CR-6	59.6	19.1	0.82	0.14	0.21	0.35	11.1	0.09	0.07	8.10	99.2
Hilaire	54.8	23.6	<0.01	<0.01	0.08	0.05	13.4	<0.01	0.03	8.45	100.4

consistent with Al-Si disorder over a single tetrahedral site. For a sample dehydrated at 1033 K for 23 h and observed at room temperature (RT), the absence of H_2O molecules distorts the tetrahedral framework, resulting in peak broadening and an increased chemical shift range (Murdoch et al. 1988).

Other NMR studies of alkali elements in aluminosilicate minerals provide a reference from which to interpret our data. These include ^{23}Na in alkali feldspar and nepheline (Phillips et al. 1988; Stebbins et al. 1989), silicates in general (Xue and Stebbins 1993), and various cations in the interlayers of clay minerals (Bank et al. 1989; Luca et al. 1989; Laperche et al. 1990; Weiss et al. 1990a, 1990b; Tinet et al. 1991; Lambert et al. 1992; Jakobsen et al. 1995; Kim et al. 1995, 1996a, 1996b).

There also have also been several published studies of Na in synthetic zeolites at various temperatures. Tijink et al. (1987) and Janssen et al. (1989) studied Na-A zeolite using ^{23}Na, ^{27}Al, and ^{29}Si NMR up to 953 K. Haase et al. (1991) studied quadrupolar nuclei (^{17}O, ^{23}Na, ^{27}Al, and ^{71}Ga) in a series of synthetic zeolites and found that T_1 relaxation is dominated overwhelmingly by modulation of the time-dependent electric field gradients due to motion of the H_2O molecules and cations in the zeolite pores.

SAMPLES AND EXPERIMENTAL METHODS

This study used two analcimes with different origins. One (CR-6) is from the Big Sandy Formation of Mohave County, Arizona, (Sheppard and Gude 1973) and was formed by diagenesis of tuffaceous rocks. It is greenish and is reported to have a high Si/Al ratio (2.3–2.8). The other sample (Hilaire) is of hydrothermal origin, is from Mont St. Hilaire, Quebec, Canada, and was obtained from Wards Natural Sciences. Its crystals are euhedral and milky or transparent. The samples used for TGA, DTA (differential thermal analysis), NMR, and XRD (X-ray diffraction) were ground in an agate mortar and pestle. Chemical compositions of the samples were determined by X-ray fluorescence (XRF) analysis at the XRAL Laboratories (Toronto, Canada).

TGA and DSC experiments were carried out with a Netzsch model STA 409 simultaneous thermal analyzer. About 30 mg of sample was used for each experiment and the same amount of Al_2O_3 was used for the reference. The temperature was increased at 5 °C/min from 20 to 1000 °C under a nitrogen atmosphere.

All NMR spectra were collected using a home-built NMR spectrometer with a superconducting solenoid magnet (8.45 T) and Nicolet 1280 computer system. Room- and high-temperature static ^{23}Na and ^{27}Al NMR spectra were collected with Larmor frequencies (ω_0) of 95.2 MHz for ^{23}Na and 93.7 MHz for ^{27}Al using a Doty high-temperature probe, which is capable of magic angle spinning (MAS) and static operation up to 700 °C. Normally 1 ms pulses were used (solid Al $\pi/2$ = 5–9 μs and Na 9–13 μs) with delays of 1 to 2 s. A quartz glass tube with a 3 mm hole in one end closed with a glass fiber was used for the sample holder to allow H_2O to escape at high temperature but to protect the sample from flowing gas. The sample temperature was controlled by heating N_2 gas in a resistance heater located just above the sample. The temperature was monitored by a thermocouple located in the heater about 4 cm above the sample. Above 300 °C Ar was used instead of N_2. The uncertainty in the temperature measurement was ±5 °C. A time delay of at least 10 min was used between collection of each spectrum to allow thermal equilibrium. Spectra collected at the same temperature over a period of several hours at each temperature do not change noticeably, indicating that the H_2O content of the analcime is constant (Line et al. 1995). The ^{27}Al and ^{23}Na chemical shifts are reported in parts per million (ppm) from external 1M $AlCl_3$ and 1M NaCl solutions.

The ^{23}Na and ^{27}Al T_1 values for both samples were obtained with a 1024-pulse saturating comb pulse sequence spaced at 5 ms ($\gg T_2$) to set the z-magnetization to 0, followed by a delay τ (0.1 ms to 20 s) and a single $\pi/6$ sampling pulse. Each T_1 value was obtained by a fit of 15 to 20 different τ values.

Room- and high-temperature ^{29}Si MAS NMR spectra were collected with the same probe and magnet at a Larmor frequency of 71.4 MHz. Pulses of $\pi/4$ ($\pi/2$ = 14 ms for TMS) with a delay of 0.5–20 s were used. An open MAS rotor was used to allow H_2O to escape at high temperature. The spinning speed was about 2 kHz. N_2 and Ar were used for sample spinning and heating. High-temperature ^{29}Si MAS spectra were collected for only sample CR-6, because the T_1 of the Hilaire sample was too long to provide adequate signal-to-noise ratios at high temperature. The ^{29}Si chemical shifts are reported in parts per million from external tetramethyisilane (TMS).

RESULTS AND DISCUSSION

Chemical composition

The chemical compositions of the two samples are slightly different (Table 1), with the main differences being their Si, Al, and Na contents. Sample CR-6 has a Si/Al atomic ratio of 2.63 whereas the Hilaire sample has a Si/Al ratio of 1.97. The Si/Al ratio of CR-6 is in the range for analcime from the Big Sandy Formation (Sheppard and Gude 1973). As is typical of hydrothermal anal-

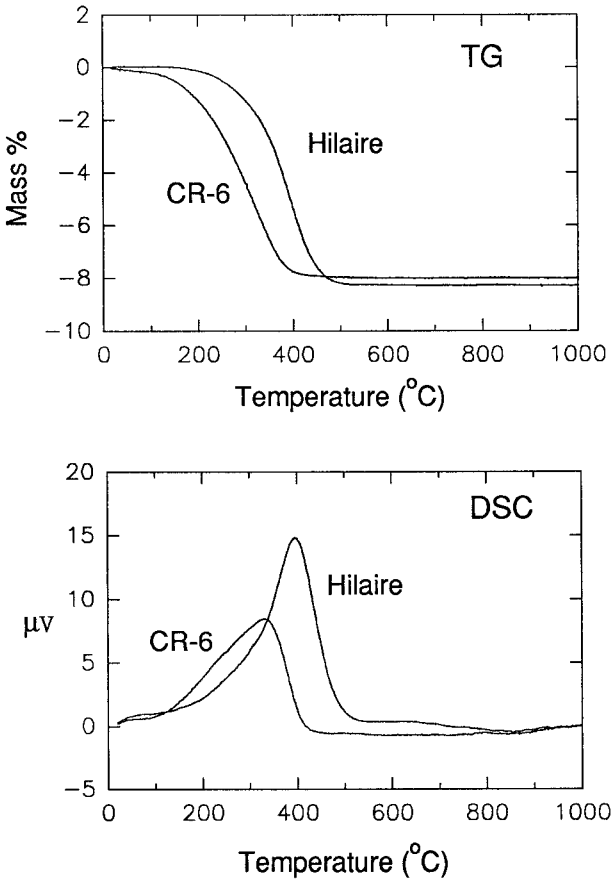

FIGURE 1. TG (**top**) and DSC **(bottom**) data from 20 to 1000 °C for the CR-6 and Hilaire analcime samples.

cimes, the Si/Al ratio of the Hilaire sample is essentially the stoichiometric value of 2. CR-6 has 0.82 wt% Fe_2O_3(T), whereas the Hilaire sample is essentially Fe free. It also has lower concentrations of all other cations except Na_2O.

TGA and DSC

The two samples show qualitatively similar but quantitatively different TGA and DSC features related to dehydration at high temperature (Fig. 1). For sample CR-6 the main H_2O loss starts near 150 °C and is complete near 400 °C. For the Hilaire sample dehydration begins near 250 °C and is complete near 480 °C. The temperature range over which the main H_2O loss occurs is larger for sample CR-6. As a result the endothermic DSC peak for sample CR-6 has a larger width and is at lower temperatures than that of the Hilaire sample.

Similar differences in the dehydration of various analcimes have been observed previously for a hydrothermal analcime and Na-exchanged leucite by Giampalo and Lombardi (1994) and Line et al. (1995). Line et al. (1995) attributed the different dehydration temperatures to different specific surface areas, with samples having larger surface areas dehydrating at lower temperatures. Surface

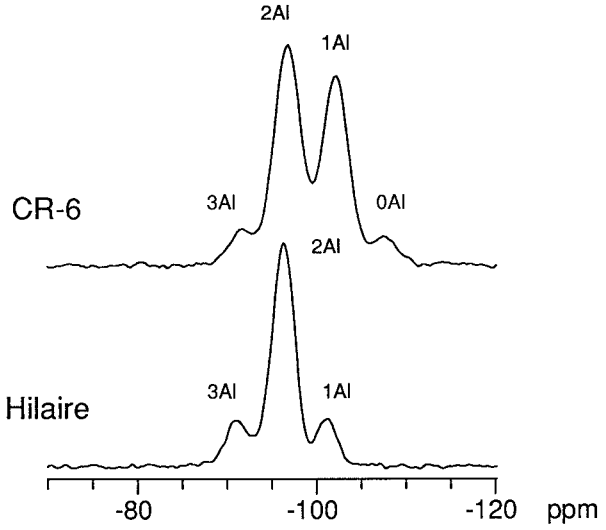

FIGURE 2. Room-temperature MAS ^{29}Si NMR spectra for the CR-6 and Hilaire analcime samples.

area difference is probably also the main reason for the different dehydration behavior of our samples. Sample CR-6 consists of subhedral to euhedral crystals with sizes from 5 to 50 μm (Sheppard and Gude 1973). The Hilaire sample was crushed from large crystals, and the optically observed average diameter of the particles is estimated to about three times as large as that of the CR-6.

On dehydration, the CR-6 and Hilaire samples lose 8.00 and 8.29 wt% H_2O, respectively. These values are very close to the loss-on-ignition (LOI) values of 8.10 and 8.45 wt% (Table 1). This result is contrary to a previous report that H_2O content increases with increasing Si/Al ratio (Breck 1984). The reason for this difference is not clear.

^{29}Si NMR spectra

The ^{29}Si spectra of the two analcime samples show several peaks due to Q^4 tetrahedrally coordinated Si with next nearest neighbor (NNN) Al atoms from zero to three (Fig. 2). Sample CR-6 has four peaks at −107.3, −102.0, −96.8, and −91.7 ppm corresponding to Q^4(0Al) to Q^4(3Al), and the Hilaire sample has three peaks at −101.2, −96.3, and −91.3 ppm corresponding to Q^4(1Al) to Q^4(3Al). Due to the different Si/Al ratios of the samples, the four peaks have different relative intensities, and the −107.3 ppm peak is missing for the Hilaire sample. The chemical shift range for each type of site is large for a zeolite with one tetrahedral site (Engelhardt and Michel 1987). Assuming that there are no Al-O-Al linkages in the framework, the Si/Al ratio can be calculated from the ^{29}Si MAS spectra (Engelhardt and Michel 1987; Kirkpatrick 1988) using the relationship

$$\text{Si/Al} = \frac{\sum_{n=0}^{4} I_{\text{Si}(n\text{Al})}}{\sum_{n=0}^{4} (n/4) I_{\text{Si}(n\text{Al})}}$$

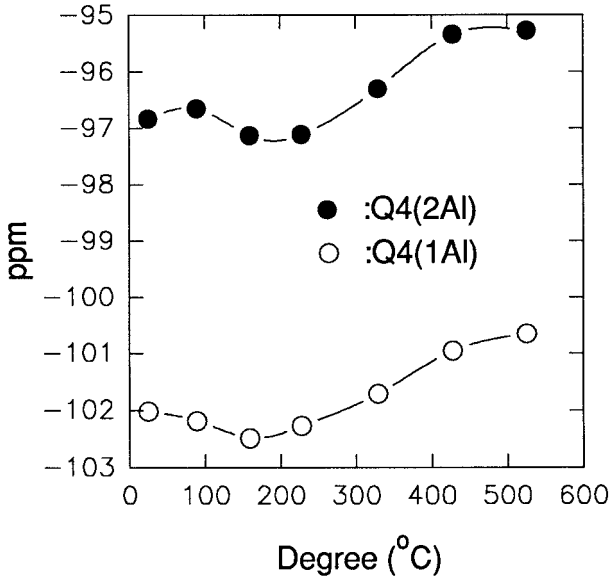

FIGURE 3. The ^{29}Si NMR chemical shifts for the Q^4(1Al) and Q^4(2Al) sites of the CR-6 analcime sample with increasing temperature.

where *I* is the relative peak intensity and *n* is the number of Al tetrahedra linked to that Si tetrahedron. Using this method, the Si/Al ratio of the Hilaire sample is 1.97 and that of CR-6 is 2.60, in good agreement with the XRF results of 1.97 and 2.63. This result indicates that there is no significant concentration of Al-O-Al linkages in our analcimes, in agreement with previous works on zeolites (Engelhardt and Michel 1987; Melchior et al. 1995).

The ^{29}Si chemical shifts of the Q^4(1Al) and Q^4(2Al) peaks of the CR-6 sample become more shielded (more negative) with increasing temperature up to 150 °C and then become less shielded (less negative) up to 450 °C (Fig. 3). Only the Q^4(1Al) and Q^4(2Al) peaks have adequate S/N ratios to allow accurate determination of their positions at high temperature. The ^{29}Si NMR chemical shifts of framework silicates are closely related to the mean Si-O-T (T = Si,Al) bond angle per tetrahedron, with the values becoming more shielded with increasing angle (Engelhardt and Michel 1987; Kirkpatrick 1988; Sternberg and Priess 1993). Thus, the increasing shielding from room temperature to near 150 °C indicates that the mean Si-O-T angles become larger and the decreasing shielding at high temperatures indicates that they become smaller. The chemical shift changes of −0.5 and 2 ppm at low and high temperature correspond to changes in Si-O-T angle of −0.3° and 1.2°, respectively (Engelhardt and Michel 1987). These bond angle changes are probably caused by the combined effects of thermal expansion, distortion of the framework due to dehydration, and probably by RUMs (rigid unit modes, Line 1995). RUMs are vibrational modes in which tetrahedra rotate rigidly about the linking O atoms, causing the time-averaged bond length to decrease with increasing temperature.

Thermal expansion of framework silicates should be accommodated primarily by increasing Si-O-T bond angles with little change in the T-O distances or O-T-O angles. If the composition and structure of the counter ions and zeolitic H_2O do not change, we expect this thermal expansion to be the main control of the Si-O-T bond angles and ^{29}Si chemical shifts. At temperatures where H_2O is lost, however, we expect the framework to collapse slightly. The TG and DSC data (Fig. 1) support this interpretation, because H_2O loss does not start until 150 °C, the temperature at which the ^{29}Si chemical shifts begin to become slightly less shielded. Between ~150 and 450 °C, the effects of dehydration and RUMs appear to dominate those of simple thermal expansion, but above ~450 °C the chemical shifts change less because dehydration is complete. Line (1995) used neutron diffraction data to calculate unit-cell parameters for analcime with increasing temperature and also found that there is a slight increase in cell length below 200 °C and a fairly large decrease above 300 °C. In her work, the maximum cell length occurs between 100 and 200 °C, which is close to the temperature at which the ^{29}Si chemical shifts begin to become less shielded. For spectra collected with decreasing temperature, the chemical shift remains 0.3–0.8 ppm less shielded at a given temperature relative to data collected with increasing temperature (data not shown), indicating that the structure is slightly distorted by dehydration. We interpret the increasing shielding at ^{29}Si with decreasing temperature to indicate that the effect of RUMs is larger in the high-temperature range than thermal expansion, which causes the chemical shift to become less shielded with decreasing temperature.

^{23}Na NMR spectra

The static ^{23}Na spectra for the two samples show qualitatively similar changes in peak shape, width, and maxima with increasing temperature, with the differences paralleling the different temperatures of dehydration observed with TGA and DSC (Fig. 4). The RT ^{23}Na NMR spectra of the two samples are similar, with maxima near −5 ppm and a tail to more negative values. There are no well-defined singularities, consistent with a range of quadrupole coupling constants (QCC), chemical shift anisotropies (CSA) and isotropic chemical shifts due to tetrahedral Al,Si disorder. With increasing temperature the peak maxima first become more negative then less negative (Figs. 4 and 5). For sample CR-6 the most negative value occurs at 340 °C, and for the Hilaire sample near 430 °C. The peak widths show more complicated behavior. The RT ^{23}Na full width at half height (FWHH) of sample CR-6 (105 ppm) is slightly larger than that of the Hilaire sample (93 ppm), probably due to the presence of paramagnetic elements (mostly Fe; Table 1, Figs. 4 and 5). Near 100 °C the peaks for both samples begin to narrow, and at 220 to 250 °C for CR-6 and near 300 °C for the Hilaire sample, they are quite narrow (25–40 ppm). As temperature increases further, the peaks become broader and have maximum widths of approximately 100

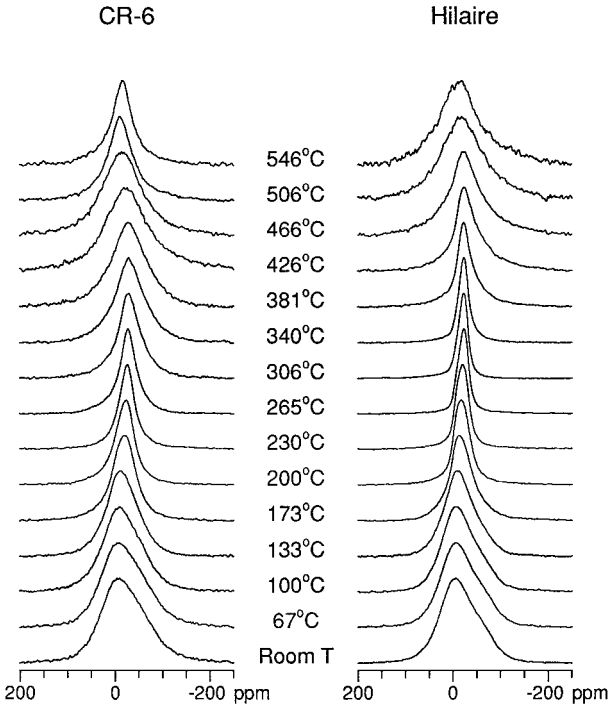

FIGURE 4. Room- and high-temperature static ^{23}Na NMR spectra for the CR-6 and Hilaire analcime samples.

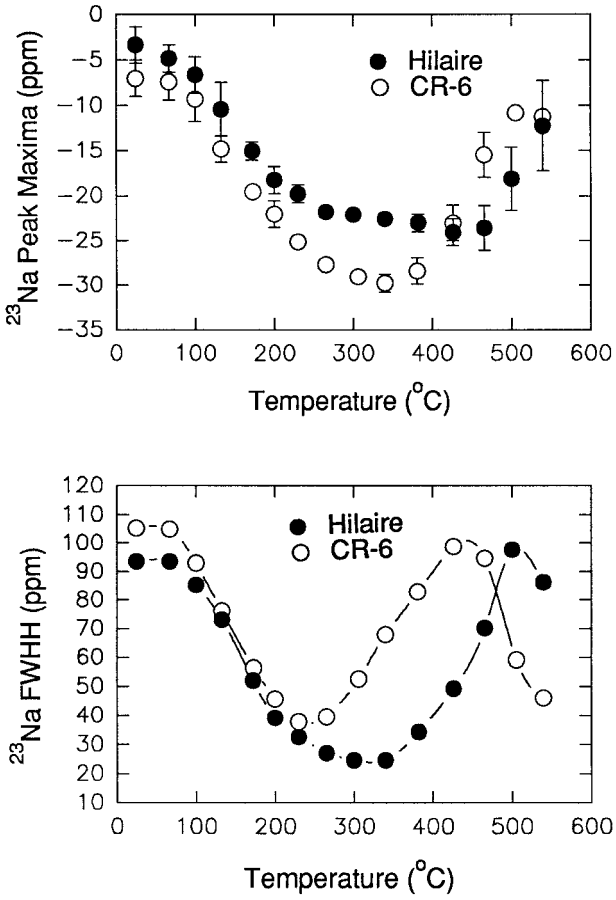

FIGURE 5. Variation of the ^{23}Na NMR peak maxima (**top**) and peak widths (FWHH) (**bottom**) with increasing temperature for the CR-6 and Hilaire analcime samples.

ppm near 440 to 450 °C for CR-6 and near 500 °C for the Hilaire sample. At higher temperatures they again decrease.

The changes in peak maxima can be explained readily in terms of changes in the nearest neighbor (NN) coordination of the Na and the Na-O distance, and by averaging of quadrupolar effects caused by Na motion. The chemical shifts of Na are correlated with the O coordination number, Na-O distance, and framework polymerization (Phillips et al. 1988; Xue and Stebbins 1993), with increasing coordination (longer Na-O distance) causing more shielded ^{23}Na chemical shifts for a given framework polymerization. For analcime, the RT peak maximum of −5 ppm is consistent with the known sixfold-coordination in the 24(c) sites, and the most negative peak maximum of −30 ppm is consistent with 12-fold coordination in the 16(b) sites. The most negative value of −25 ppm for the Hilaire sample is less negative than that of sample CR-6 and is consistent with incomplete dehydration of this coarser-grained sample. The temperatures for the most negative ^{23}Na peak maxima correlate well with the dehydration temperatures observed by TGA and DSC (Figs. 1 and 5), indicating that the changes in peak maxima are related to coordination changes caused by H_2O loss. The observation can be reconciled in the following way. As dehydration occurs, H_2O molecules leave the 16(b) sites, leaving the Na in the 24(c) sites with an average lower coordination (fourfold-coordination if both H_2O molecules are missing). Na is less stable in such sites and migrates to larger sites in the cavity. These may be the 16(b) H_2O sites, which correspond to the 12-fold coordinated K site in leucite. Based on high-temperature neutron diffraction data, Line (1995) also reported that Na leaves the 24(c) sites at temperature above 400 °C. Thus, the progressively more negative peak maximum with increasing temperature indicates progressively increasing occupancy of the larger sites. Similar more negative ^{23}Na positions occur with increasing NN coordination and Na-O distance in Na,K feldspar as K substitutes for Na (Phillips et al. 1988).

The combined decreasing peak widths and more negative peak maxima with increasing temperature are understood readily in terms of motional averaging of Na atoms among sites at 100 °C and higher. If progressively more of the Na atoms occupy the larger site but do not undergo motional averaging, the observed peak shape would be the sum of the signal from Na atoms in both sites. Thus, the peak maximum would become more negative, but the width would increase. The observed peak narrowing is thus not compatible with a static distribution of Na atoms over different sites but is fully consistent with dynamical site exchange that also averages the first-

and second-order quadrupole broadening (George and Stebbins 1996). With increasing temperature, increasing frequency of motion first averages peak broadening effects with characteristic widths in the kHz range (e.g., second-order quadrupolar effects on the ½,-½ transition), causing the narrowing in the 100 to 300 °C range. Taking the frequency of motion at the temperature where the peak is one-half the static width to be on the order of the static width gives exchange frequencies of ca. 10 kHz and 8.5 kHz for CR-6 and Hilaire near 180 °C. Because the peak maximum is proportional to the weighted average of the site occupancies, the progressively more negative ^{23}Na peak maximum from RT to 350 °C for sample CR-6 and the RT to 430 °C for the Hilaire sample indicate that the average coordination number increases with increasing temperature.

Once the frequencies of motion reach the MHz range at higher temperature, averaging of the ±(½, ⅔) transitions becomes significant, and incorporation of signal intensity due to these satellite transitions first causes peak broadening and finally peak narrowing. It also moves the peak maxima to higher frequencies due to the removal of the second-order quadrupolar shift.

Similar changes in peak maxima with increasing temperature occur for ^{23}Na in Na-silicate glass (George and Stebbins 1996) and ^{11}B in borate glasses (Inagaki et al. 1993). George and Stebbins (1996) interpret the initial decrease in frequency at ^{23}Na in their Na-silicate glass to indicate that Na explores larger sites (more negative chemical shifts) as diffusion becomes significant. They also interpret the observed increase in frequency at higher temperature to indicate averaging of the signal due to the satellite transitions. These interpretations are essentially the same as ours, except that analcime loses H_2O simultaneously and large cage sites become available for Na occupancy.

The results of ^{23}Na nutation experiments for our samples verify this interpretation. Nutation experiments measure signal intensity as a function of pulse length. For a quadrupole nucleus with spin $I = 3/2$, the maximum signal intensity occurs after a $\pi/4$ pulse (compared from $\pi/2$ pulse of liquid) if only the (½,-½) transition is excited and observed (selective), whereas it occurs after a $\pi/2$ pulse if all transitions are excited and observed (nonseletive; Fenzke et al. 1984). Under our experimental conditions all transitions are excited and observed if the QCC is close to 0. Because the Na sites of most silicate phases have quadrupole coupling constants >1 MHz, they show selective excitation. If there is atomic motion at frequencies on the order of the quadrupole coupling constant, the satellite transitions are averaged and the maximum intensity occurs for a $\pi/2$ pulse. For sample CR-6, the room-temperature ^{23}Na maximum intensity occurs at a pulse length of $\pi/4$ (selective excitation), and the pulse length with maximum intensity increases by factors of 1.1, 1.5, and 1.8 at temperatures of 130, 260, and 380 °C. Thus progressively more of the satellite intensity is observed with increasing temperature. In contrast, for albite at these same temperatures there is no significant change in the $\pi/4$ pulse length for maximum intensity in this temperature range, as also observed by George and Stebbins (1996). Thus, at 380 °C, at which sample CR-6 has the broadest high-temperature peak, the frequency of Na motion is in the MHz range, all transitions are nearly fully averaged, and the line broadening is due to nearly complete incorporation of signal from the satellite transitions in to the observed peak. At temperatures higher than this, the peak narrows as the frequency of motion increases further. The observed increased frequency of the peak maximum at higher temperature is due to isotropic averaging of the second quadrupolar coupling, which make the peak position more negative than the isotropic chemical shift (George and Stebbins 1996). This line broadening and decreased frequency can also be explained by life time broadening or multiexponential quadrupolar relaxation (Hasse et al. 1991; Inagaki et al. 1993). For these explanations to be correct, the frequency of Na motion must be on the order of the Larmor frequency (95.2 MHz), but the nutation experiment shows that this frequency is one or two orders of magnitude less than the Larmor frequency at the temperature of maximum peak width. Thus the observed effects are due to incorporation of intensity from the satellite transitions. Like the ^{29}Si results, the increasing ^{23}Na peak widths beginning at 250 °C for CR-6 but at 330 °C for the Hilaire sample are well correlated with the lower temperature of dehydration for sample CR-6.

Mobile Na in analcime at high temperature has also been suggested by Line (1995) based on neutron diffraction data. Her data show that with increasing temperature the 16(b) H_2O sites are vacated first and then the 24(c) Na sites. She could not locate the Na positions near 800 °C and concluded that Na is mobile over several sites. This observation combined with our NMR data can only be reconciled by dynamical effects with Na exploring many sites in the cage, possibly including the 24(c) sites. Similar mobility for Na at high temperature has been observed between the two large cation sites in nepheline (Stebbins et al. 1989).

The RT ^{23}Na spectra of the samples heated to 550 °C confirm that dehydration plays an important role in the high-temperature behavior of analcime. These spectra are broader than the RT spectra of the unheated samples (FWHH = 127 ppm for CR-6 and 162 ppm for Hilaire), consistent with larger average QCC values and a range of Na sites.

The ^{23}Na T_1 relaxation times (Fig. 6) could not be measured at temperatures greater than 300 °C because the values become extremely short ($<10^{-4}$ s). Thus, the relaxation mechanisms are difficult to evaluate. Paramagnetic relaxation may contribute, but because of the observed line shape changes, fluctuating electric field gradients (efg) due to Na motion probably dominate.

^{27}Al NMR spectra

The ^{27}Al spectra (Fig. 7) for the two samples show similar changes in peak shape, width, and maxima with

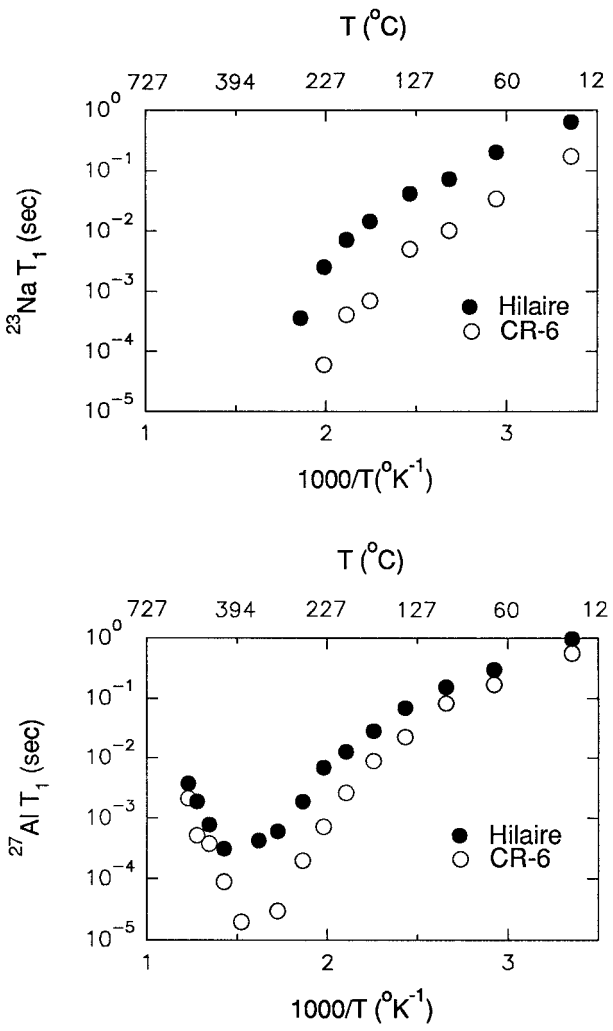

FIGURE 6. Temperature dependence of the ^{23}Na and ^{27}Al T_1 relaxation times for the CR-6 and Hilaire analcime samples.

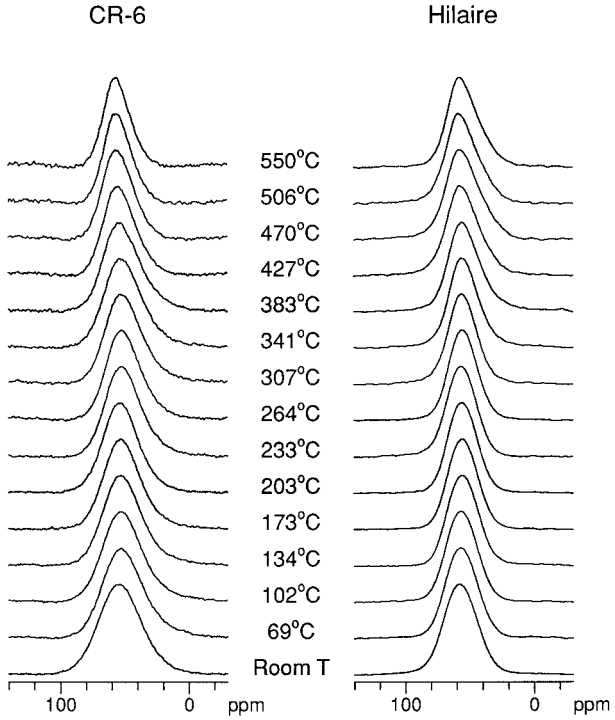

FIGURE 7. Room- and high-temperature static ^{27}Al NMR spectra for the CR-6 and Hilaire analcime samples.

increasing temperature, and as for ^{29}Si and ^{23}Na the differences parallel the dehydration observed by TGA and DSC. The static RT ^{27}Al NMR spectra of both samples contain single peaks that are only slightly asymmetrical with a tail to more shielded values. This small tail is due to second-order quadrupolar interaction, and this effect, dipolar interactions, chemical shift anisotrop (CSA), and site heterogeneity contribute to cause a relatively featureless peak. The peak maxima are 58.0 ppm for the Hilaire sample and 56.2 ppm for CR-6, in the range for $^{[4]}$Al sites in framework aluminosilicates (Engelhardt and Michel 1987; Kirkpatrick 1988; Kirkpatrick and Phillips 1993). Because of (Al,Si) tetrahedral site disorder, it is not possible to determine isotropic chemical shifts well from either MAS or static spectra. The temperature variation of the ^{27}Al static peak maximum, however, is the same as that of the ^{29}Si chemical shifts, becoming shielded then deshielded with increasing temperature (Fig. 8). The ^{27}Al chemical shifts are known to vary with mean Al-O-Si angle in a way similar to ^{29}Si chemical shifts (Engelhardt and Michel 1987; Kirkpatrick and Phillips 1993). As with the ^{29}Si results, changes in ^{27}Al are correlated to changes due to thermal expansion, dehydration, and RUMs and the resultant cell parameter changes (Fig. 8).

The ^{27}Al NMR peak widths (FWHH) are larger for CR-6 than for Hilaire, probably due to a larger paramagnetic line broadening (Oldfield et al. 1983; Smith et al. 1983, Figs. 7 and 8). With increasing temperature the ^{27}Al peak widths for sample CR-6 decrease up to 270 °C, increase again, and above 350 °C decrease again. The trend for the Hilaire sample is similar, but the increasing peak width occurs at a higher temperature than for sample CR-6. The decrease of peak widths at low temperature can be explained by dynamical effects caused by movement of H_2O and Na in the channels at frequencies >20 kHz, and the resulting decrease of the time-averaged ^{27}Al QCC. The peak width increase at higher temperature is correlated to the loss of water, which distorts the framework, causing more distorted Al environments with increasing quadrupole coupling constants and CSA values. Because sample CR-6 dehydrates at lower temperatures than the Hilaire sample, its peak width increase occurs at a lower temperature.

The ^{27}Al T_1 relaxation times for our samples behave in the classic manner, decreasing and then increasing with increasing temperature, except that the slopes above and below the T_1 minimum are not the same (Fig. 6). The T_1 values for CR-6 are shorter than for the Hilaire sample at all temperatures, probably due to the larger concentra-

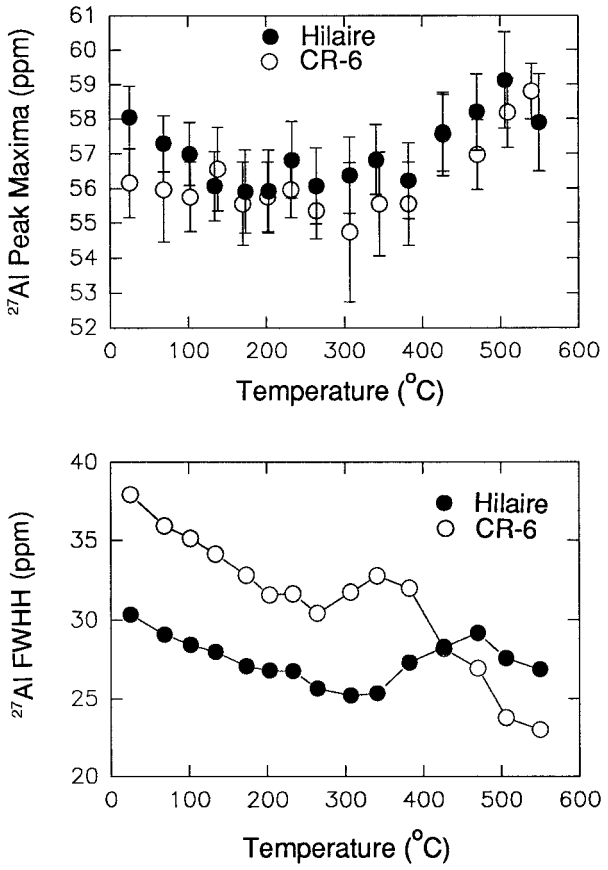

FIGURE 8. Variation of the ^{27}Al NMR peak maxima and peak widths (FWHH) with increasing temperature for the CR-6 and Hilaire analcime samples.

tion of paramagnetic impurities in CR-6 (Table 1). Relaxation to paramagnetic centers is one of the most common T_1 relaxation mechanisms in natural minerals (Basler 1985; Engelhardt and Michel 1987); it is effective at low temperatures and probably contributes to the relaxation of both samples. Paramagnetic relaxation rate increases as $T^{1/4}$, however, and thus for ^{27}Al in analcime, quadrupolar relaxation probably dominates at most temperatures. For quadrupolar nuclides, the stretched exponential coefficient c in the relationship $M(t) = Mo[1\text{-}\exp(t/T_1)^c]$ is normally less than 1 and does not show single exponential relaxation ($c = 1$) when only the central transition is excited (Hughes 1993; George and Stebbins 1996). The c values in our samples are in the range 0.2 to 0.6 indicating either that the ^{23}Na QCC is large for our samples and not fully averaged in our temperature range or that more than one relaxation mechanism exists (or both). Hasse et al. (1991) investigated the T_1 behavior for a series of synthetic zeolites and reported that their T_1 relaxation is dominated overwhelmingly by modulation of the time-dependent electric field gradient due to motion of H_2O molecules and cations in the zeolite pores. Several relaxation models, including phonon-based relaxation models for quadrupolar elements, show that in general, minimum T_1 values are inversely proportional to QCC^2 (Hasse et al. 1991). For our samples, the ^{27}Al T_1 values are longer than those for ^{23}Na, even though the ^{27}Al QCC values are larger than those of motionally averaged Na at high temperature. Hasse et al. (1991) observed similar results and suggested a model involving a fluctuating efg [eq(t)] caused primarily by motion of H_2O molecules. For our ^{27}Al results this mechanism probably contributes below the temperature of complete dehydration. Above this temperature ^{23}Na motion may become important. If Na motion were the dominant mechanism for ^{27}Al T_1 relaxation, however, the ^{27}Al T_1 minima should occur at temperatures higher than that at which the broadest ^{23}Na peaks occur, because the Larmor frequency is $\gg$ QCC. However, our ^{27}Al T_1 minima occur at temperatures slightly lower than those of maximum ^{23}Na peak widths, indicating at least that this is not the only mechanism operating. Thus, as for the other NMR parameters observed here, ^{27}Al T_1 relaxation is controlled by H_2O motion and loss and the resultant structural changes. The apparent activation energies for ^{27}Al T_1 at temperatures above the minima are slightly different (123 kJ/mol and 103 kJ/mol for CR-6 and Hilaire) probably due to their different dehydration behaviors or their different chemical compositions and resultant different structures.

ACKNOWLEDGMENTS

The authors appreciate the detailed comments of the reviewers Anna George, Simon Kohn, and Jonathan Stebbins for the final manuscript. This work was sponsored by NSF grants EAR 93-15695 and 95-26317 (R.J.K., P.I.). We also thank Richard L. Hay for providing the CR-6 sample.

REFERENCES CITED

Bank, S., Bank, J.F., and Ellis, P.D. (1989) Solid-state ^{113}Cd nuclear magnetic resonance study of exchanged montmorillonites. Journal of Physical Chemistry, 93, 4847–4855.

Basler, W.D. (1985) ^{7}Li-NMR relaxation of hydrated zeolite Li-X. Journal of Chemical Physics, 82, 5297–5298.

Breck, D.W. (1984) Zeolite Molecular Sieves. Robert E. Krieger Publishing Company, Malabar, Florida.

Dyer, A. and Molyneux, A. (1968) The mobility of water in zeolites-I: Self-diffusion of water in analcime. Journal of Inorganic and Nuclear Chemistry, 30, 829–837.

Dyer, A. and Yusof, A.M. (1987) Diffusion in heteroionic analcimes: Part 1.Sodium-potassium-water system. Zeolites, 7, 191–196.

———(1989) Diffusion in heteroionic analcimes: Part II. Diffusion of water in sodium/thallium, sodium/lithium, and sodium/ammonium analcimes. Zeolites, 9, 129–135.

Engelhardt, G. and Michel, D. (1987) High-resolution solid-state NMR of silicates and zeolites. Wiley, New York.

Fenzke, D., Freude, D., Fröhlich, T., and Hasse, J. (1984) NMR intensity measurements of half-integer quadrupole nuclei. Chemical Physics Letters, 111, 171–175.

Ferraris, G., Jones, D.W., and Yerkess, J. (1972) A neutron-diffraction study of the crystal structure of analcime, $NaAlSi_2 \cdot H_2O$. Zeitschrift für Kristallographie, 135, 240–252.

Garney, B.W. (1992) Development of the zeolite analcime for tritiated water storage. Fusion Technology, 21, 604–611.

George, A.M. and Stebbins, J.F. (1996) Dynamics of Na in sodium aluminosilicate glasses and liquids. Physics and Chemistry of Minerals, 23, 526–534.

Gottardi, G. and Galli, E. (1985) Natural Zeolites. Springer-Verlag, Berlin Heidelberg.

Haase, J., Park, K.D., Guo, K., Timken, H.K.C., and Oldfield, E. (1991)

Nuclear magnetic resonance spectroscopic study of spin-lattice relaxation of quadrupolar nuclei in zeolites. Journal of Physical Chemistry, 95, 6996–7002.

Hellner, E. and Koch, E. (1979) The oxygen framework of leucite and analcime (1). Mineralogica et Petrographica Acta, 23, 303–311.

Hughes, D.G. (1993) Non-exponential relaxation of I = 3/2 nuclear spins in solids. Journal of Physics Condensed Matter, 5, 2025–2032.

Inagaki, Y., Maekawa, H., Yokokawa, T., and Shimokawa, S. (1993) Nuclear-magnetic-resonance study of the dynamics of networking-glass-forming systems: $xNa_2O\cdot(1\text{-}x)B_2O_3$. Physical Review B, 47, 674–680.

Jakobsen, J.J., Nielsen, N.C., and Lindgreen, H. (1995) Sequences of charged sheets in rectorite. American Mineralogist, 80, 247–252.

Janssen, G.A., Tijink, G.A.H., Veeman, W.S., Maesen, T.I.M., and van Lent, J.F. (1989) High-temperature NMR study of zeolite Na-A: detection of a phase transition. Journal of Physical Chemistry, 93, 899–904.

Kim, Y., Kirkpatrick, R.J., and Cygan, R.T. (1995) ^{133}Cs NMR study of Cs reaction with clay minerals. In V. Jain and R. Palmer, Ed., Environmental Issues and Waste Management Technologies in the Ceramic and Nuclear Industries, Ceramic Transactions, 61, 629–636.

Kim, Y., Cygan, R.T., and Kirkpatrick, R.J. (1996a) ^{133}Cs NMR and XPS investigation of cesium adsorbed on clay minerals and related phases. Geochimica et Cosmochimica Acta, 60, 1041–1052.

Kim, Y., Kirkpatrick, R.J., and Cygan, R.T. (1996b) ^{133}Cs NMR study of cesium on the surfaces of kaolinite and illite. Geochimica et Cosmochimica Acta, 60, 4059–4074.

Kirkpatrick, R.J. (1988) MAS-NMR spectroscopy of minerals and glasses. In Mineralogical Society of America Reviews in Mineralogy, 18, 341–403.

Kirkpatrick, R.J. and Phillips, B.L. (1993) ^{27}Al NMR spectroscopy of minerals and related materials. Applied Magnetic Resonance, 4, 213–236.

Knowles, C.R., Rinaldi, F.F., and Smith, J.V. (1965) Refinement of the crystal structure of analcime. Indian Mineralogist, 6, 127–140.

Kohn, S.C., Henderson, C.M.B., and Dupree, R. (1995) Si-Al order in leucite revised: New information from an analcite-derived analogue. American Mineralogist, 80, 705–714.

Lambert, J-F., Prost, R., and Smith, M.E. (1992) ^{39}K solid-state NMR studies of potassium tecto- and phyllosilicates: The in situ detection of hydratable K+ in smectites. Clays and Clay Minerals, 40, 253–261.

Laperche, V., Lambert, J.F., Prost, R., and Fripiat, J.J. (1990) High-resolution solid-state NMR of exchangeable cations in the interlayer surface of a swelling mica: ^{23}Na, ^{111}Cd, and ^{133}Cs vermiculites. Journal of Physical Chemistry, 94, 8821–8831.

Line, C.M. (1995) The behavior of water in analcime, $NaAlSi_2O_6\cdot H_2O$. Ph.D Thesis, Department of Earth Science, University of Cambridge.

Line, C.M., Putnis, A., Putnis, C., and Giampaolo, C. (1995) The dehydration kinetics and microtexture of analcime from two parageneses. American Mineralogist, 80, 268–279.

Luca, V., Cardile, C.M., and Meinhold, R.H. (1989) High-resolution multinuclear NMR study of cation migration in montmorillonite. Clay Minerals, 24, 115–119.

Mazzi, F. and Galli, E. (1978) Is each analcime different? American Mineralogist, 63, 448–460.

Mazzi, F., Galli, E., and Gottardi, G. (1976) The crystal structure of tetragonal leucite. American Mineralogist, 61, 108–115.

Melchior, M.T., Vaughan, D.E.W., and Pictroski, C.F. (1995) Local environment fine structure in the ^{29}Si NMR spectra of faujasite zeolites. Journal of Phyical Chemistry, 99, 6128–6144.

Murdoch, J.B., Stebbins, J.F., Carmichael, I.S.E., and Pines, A. (1988) A silicon-29 nuclear magnetic resonance study of silicon-aluminum ordering in leucite and analcite. Physics and Chemistry of Minerals, 15, 370–382.

Oldfield, E., Kinsey, R.A, Smith, K.A., Nichols, J.A., and Kirkpatrick, R.J. (1983) High-resolution NMR of inorganic solids. Influence of magnetic centers on magic-angle sample-spinning line shapes in some natural aluminosilicates. Journal of Magnetic Resonance, 51, 325–329.

Phillips, B.L. and Kirkpatrick, R.J. (1994) Short-range Si-Al order in leucite and analcime: Determination of the configurational entropy from ^{27}Al and variable-temperature ^{29}Si NMR spectroscopy of leucite, its Cs- and Rb-exchanged derivatives, and analcime. American Mineralogist, 79, 1025–1031.

Phillips, B.L. Kirkpatrick, R.J., and Hovis, G.L. (1988) ^{27}Al, ^{29}Si, and ^{23}Na MAS NMR study of an Al, Si ordered alkali feldspar solid solution series. Physics and Chemistry of Minerals, 16, 262–272.

Sheppard, R.A. and Gude, A.J. (1973) Zeolites and associated authigenic silicate minerals in tuffaceous rocks of the Big Sandy Formation, Mohave County, Arizona. Geological Survey Professional Paper 830, 1–36.

Smith, K.A., Kirkpatrick, R.J., Oldfield, E., and Henderson, D.M. (1983) High-resolution silicon-29 nuclear magnetic resonance spectroscopic study of rock-forming silicates. American Mineralogist, 68, 1206–1215.

Stebbins, J.F., Farnan, I., Williams, E.H., and Roux, J. (1989) Magic angle spinning NMR observation of sodium exchange in nepheline at 500 °C. Physics and Chemistry of Minerals, 16, 763–766.

Sternberg, U. and Priess, W. (1993) The influence of structure and geometry on the silicon-29 chemical shift. Journal of Magnetic Resonance, 102, 160–165.

Taylor, W.H. (1930) The structure of analcite ($NaAlSi_2O\cdot H_2O$). Zeitschrift für Kristallographie, 16, 113–114.

Tijink, G.A.H., Janssen, R., and Veeman, W.S. (1987) Investigation of the hydration of zeolite NaA by two-dimensional ^{23}Na nutation NMR. Journal of American Chemical Society, 109, 7301–7304.

Tinet, D., Faugere, A.M., and Prost, R. (1991) 113Cd NMR chemical shift tensor analysis of cadmium-exchanged clays and clay gels. Journal of Physical Chemistry, 95, 8804–8807.

Todorović, M., Gal, I.J., and Brücher, H. (1987a) The exchange of tritiated water between natural zeolite analcime and surrounding water. Radioactive Waste Management and the Nuclear Fuel Cycle, 8, 339–346.

Todorović, M., Radak-Jovanović, Z., Gal, I.J., and Dyer, A. (1987b) The release of tritiated water from synthetic analcime into surrounding water. Colloids and Surfaces, 23, 345–351.

Weiss, C.A., Jr., Kirkpatrick, R.J., and Altaner, S.P. (1990a) The structural environment of cations adsorbed onto clays: ^{133}Cs variable-temperature MAS NMR spectroscopic study of hectorite. Geochimica et Cosmochimica Acta, 54, 1655–1669.

———(1990b) Variations in interlayer cation sites of clay minerals as studied by ^{133}Cs MAS nuclear magnetic resonance spectroscopy. American Mineralogist, 75, 970–982.

Xue, X. and Stebbins, J.F. (1993) ^{23}Na NMR chemical shifts and local Na coordination environments in silicates crystals, melts, and glasses. Physics and Chemistry of Minerals, 20, 297–307.

Manuscript received April 17, 1997
Manuscript accepted November 12, 1997